Int. J. Multiphase Flow, Vol. 1, pp. 123–138. Pergamon Press, 1973. Printed in Great Britain.

THE LOCAL STRUCTURE OF GAS FLUIDIZED BEDS —II. THE SPATIAL DISTRIBUTION OF BUBBLES

J. WERTHER and O. MOLERUS

Institut für Mechanische Verfahrenstechnik der Universität Erlangen-Nürnberg, 8520 Erlangen, W. Germany

(*Received* 15 *May* 1973)

Abstract—The spatial distribution of bubbles in gas fluidized beds has been investigated with the measuring system described in Part I of this paper in beds of 0.10, 0.20, 0.45 and 1.0 m dia. The results indicate that in gas fluidized beds a characteristic flow profile of the bubble phase exists such that near the distributor a zone of increased bubble development exists in an annulus near the wall. This zone moves towards the vessel centre-line with increasing height above the distributor. The merging of the annular zone in the vessel centre-line marks the beginning of the transition of the fluidized bed to the state of slugging. The spatial flow profile of the bubble phase is shown to be responsible for the existence of characteristic solids circulation patterns in gas fluidized beds.

1. INTRODUCTION

The spatial distribution of bubbles within a gas/solid fluidized bed has a considerable influence on the operation of such beds. For example, the distribution of rising bubbles over the cross-section of the bed influences the efficiency of a fluidized bed reactor because non-uniformity of bubble development over the bed cross-section causes a broadening of the residence-time distribution of the gas. The latter is brought about by a reduced residence-time, due to higher rise velocities of bubbles, in regions of more intense bubble development and also by the influence on gas mixing brought about by large scale solids movement necessarily associated with uneven bubble development

Although there exist in the voluminous fluidized bed literature many, partly contradictory, references, surveyed by Grace & Harrison (1968), to the occurrence of uneven bubble development and of solids circulation, to date no adequately accurate direct measurements are available of the spatial distribution of bubbles in three-dimensional beds. The few available measurements obtained with X-rays (Baumgarten & Pigford 1960), and with capacitive (Kunii, Yoshida & Hiraki 1967) and electroresistivity probes (Park *et al.* 1969), merely yielded the qualitative result that near the gas distributor more bubbles were found near the bed wall than at the bed centre, while at large heights above the distributor the reverse held. The same results were indicated by the experiments of Whitehead & Young (1967) who photographed bubble eruptions at the surface of large-scale fluidized beds. These workers established that at the bed surface an eruption pattern was clearly distinguishable, and that this pattern varied significantly with bed height. One of the first systematic quantitative investigations of the spatial distribution of bubbles in a fluidized bed was carried out by Grace & Harrison (1968) by means of photographing bubbles in a two-

dimensional bed. The development of a characteristic non-uniformity in the bubble distribution across the bed was interpreted by means of a simple coalescence model.

The measuring techniques described in Part I of this paper allow an exact observation of the bubble development in three dimensional beds of arbitrary dimensions. The investigations of the spatial distribution of bubbles in cylindrical beds of from 0.10 to 1.0 m dia. showed that gas/solid fluidized beds are basically characterized by a non-uniform bubble development across the bed cross-section, so much so that one may talk of a "spatial flow profile of the bubble phase". The existence of the flow profile of the bubble phase is decisive in the transition of the bed to the state of slugging and is closely connected with the development of the solids circulation within the bed.

2. EXPERIMENTAL

Three solids, whose sieve-analyses are shown in figure 1, were used. Their properties were as follows:

(i) quartz sand: irregular particle shape, density $\rho_s = 2640\ \text{kg/m}^3$, minimum fluidization velocity $u_{mf} = 0.018$ m/sec;
(ii) copper powder: spherical particle shape, density $\rho_s = 8660\ \text{kg/m}^3$, $u_{mf} = 0.014$ m/sec;
(iii) glass spheres: $\rho_s = 2950\ \text{kg/m}^3$, $u_{mf} = 0.039$ m/sec.

Figure 2 shows a schematic representation of the experimental rig. Air, used as the fluidizing agent, was circulated in a closed loop by a rotary compressor. The hydrodynamics of fluidization was investigated in cylindrical vessels of 0.10, 0.20, 0.45 and 1.0 m dia. Sintered metal plates with a mean pore size of 5 μm were used as distributors in the beds of 0.10, 0.20 and 1.0 m dia. while in the bed of 0.45 m dia. a porous plastic plate with a mean pore size of 40 μm was used. The removal of fines carried over in the outlet gas stream was effected by downstream cyclones. The air flow was measured by rotameters for the two smaller beds and with orifice plates for the larger beds.

The electronic data processing set-up is shown schematically in figure 3. In the investigation of the local state of fluidization within a fluidized bed, the probability density distribution $w(U_A)$ of the amplitudes of the output signal $U_A(t)$ arising from probe A. was first measured by a Hewlett–Packard 3721A correlator. Then the signal $U_A(t)$ was displaced

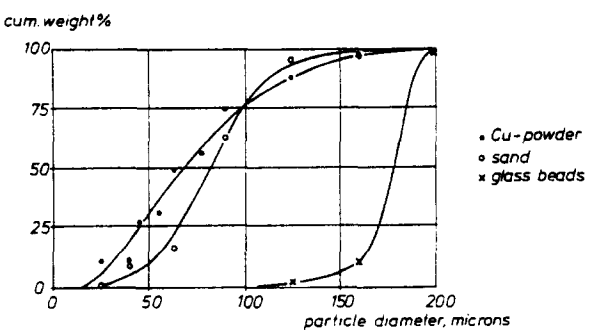

Figure 1. Sieve analyses of the materials used.

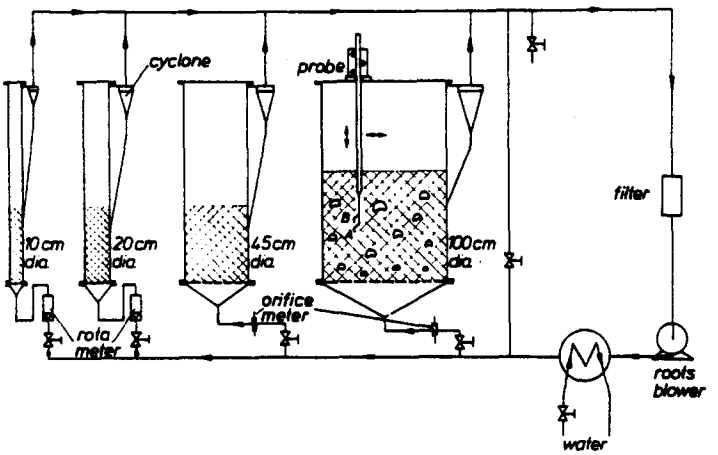

Figure 2. Schematic representation of the experimental rig.

relative to the reference voltage of the discriminator circuit by means of an offset-voltage such that the output signal $U'_A(t)$ of the discriminator circuit contained no component due to the dense phase porosity fluctuations, but only the complete series of the "cut" bubble pulses. This was done in accordance with the principles established in Part I of this paper. The accuracy of the adjustment was controlled by a measurement of the amplitude distribution $w(U'_A)$ of the cut signal $U'_A(t)$. The signal arising from the lower probe, $U_B(t)$, was modified in the same way. Subsequently, the cross-correlation function $\phi_{U'_A U'_B}(\tau)$ of the two bubble pulse series $U'_A(t)$ and $U'_B(t)$ was measured by means of a correlator whence, the local mean bubble rise velocity $\bar{v}_b$ was determined. The timing circuit as well as the two electronic counters were used to determine the mean number k of bubbles striking probe A per unit time and the mean duration $\bar{t}_b$ of the bubble pulses. The following parameters were then determined:

the local mean pierced length of bubbles, $E[l] = \bar{v}_b \bar{t}_b$; [1]

the local mean bubble volume fraction, $\bar{\varepsilon}_b = k\bar{t}_b$; [2]

and the local bubble gas flow, $\dot{V}_b = k\bar{t}_b\bar{v}_b$. [3]

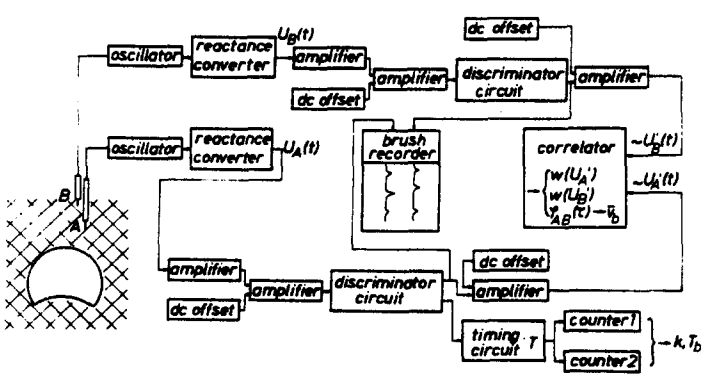

Figure 3. Electronic data processing set-up.

Using a total measuring time of about 20 min, during which each probe has been struck by between 1000 and 5000 bubbles, one obtained very accurate, statistically certain, information about the local state of fluidization. No curve-fitting techniques were used in representing the data in the following figures.

3. RESULTS AND DISCUSSION

3.1. *The spatial distribution of bubbles in a non-slugging fluidized bed*

The investigation of the spatial distribution of bubbles within a fluidized bed was carried out as follows. Initially the bubble development was observed at fixed height above the gas distributor. Conclusions about the spatial distribution of bubbles were then drawn from a comparison of the bubble development over bed cross-sections at different heights.

The immediately obvious parameter for the investigation of the uniformity of bubble development was k, the mean number of bubbles that struck the probe per unit time. As an example, figure 4 shows the number k versus the distance r from the vessel center line, in a 0.20 m dia. fluidized bed of sand at a height 0.15 m above the distributor.

The parameter k must not, however, be confused with the local bubble frequency f, defined as the number of bubble centres passing a unit cross-sectional area around the probe per unit time. For spherical bubbles rising randomly in space relative to the probe, simple reasoning (Werther, 1973) leads to the relation

$$k = \frac{\pi f}{4} \int_{D_{min}}^{D_{max}} D^2 q_o(d)\, dD \qquad [4]$$

where D is the diameter of spherical bubble, $D_{min} \leq D \leq D_{max}$ and $q_o(d)$ is the local number density distribution of the diameters D.

Due to the different cross-sectional areas that bubbles of different sizes present to the probe, the profile $k(r)$ is only suited to the characterization of the uniformity of bubble development over the bed cross-section, providing the local bubble size distribution is

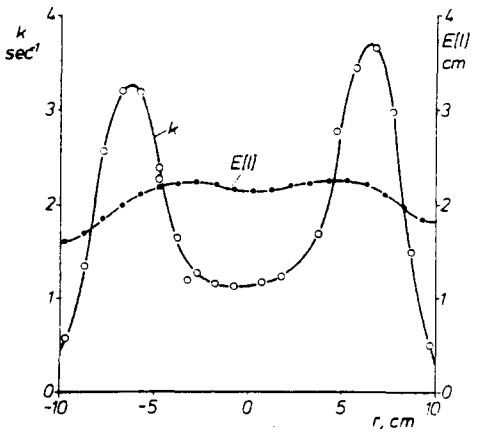

Figure 4. Local mean number of bubbles striking the probe per unit time, and local mean bubble pierced length versus the radial displacement of the probe from the column centre-line (0.20 m dia. sand fluidized bed, gas velocity 0.09 m/sec, probe located 0.15 m above the distributor).

independent of distance r from the vessel centre-line. In figure 4 measurements of the local mean pierced length $E[l]$ at various points of the bed cross-section, showed that this is not the case. Furthermore, the coupling of the measured magnitude k with the sizes of the bubbles, complicates a direct comparison of the $k(r)$ profiles measured at different heights above the distributor. By contrast, the local bubble gas flow $\dot{V}_b$ is considerably more suited to the determination of the uniformity of bubble development over a bed cross-section. Using the parameter $\dot{V}_b$ the bubbles may be viewed as a dispersed phase flowing through the bed according to a distribution given by the magnitude of $\dot{V}_b$. This distribution is suited for the spatial description of the bubbles, in particular with reference to the large scale solids circulation that is set up within the bed.

In figure 5 measurements of $\dot{V}_b$ are shown as a function of the distance r from the vessel centre-line in the 0.20 m dia. fluidized bed of sand, at heights of 0.05, 0.08 and 0.15 m above the distributor. In spite of uniform permeability of the distributor and in spite of a high ratio of distributor pressure drop p_D to bed pressure drop $p_B(p_D/p_B = 3.8$ for the sintered metal distributor) it is evident that bubble development is not uniform over the bed cross-section. Rather one finds near the distributor an annular zone close to the wall of pronounced bubble development. In addition it is found that the flow profiles change such that the annular zone converges to the vessel centre with increasing height.

Similar flow profiles of the bubble phase result with other solids, as is shown in figures 6 and 7 for glass spheres and copper powder in fluidized beds of 0.20 m dia.

In figure 8 the bubble development in a fluidized bed of sand with a diameter of 0.45 m is shown. The porous plastic distributor used exhibits a low pressure drop relative to that of the bed ($p_D/p_B = 0.2$) without changing the flow profile of the bubble phase.

The occurrence of a zone of increased bubble development near the wall is not confined to small laboratory scale fluidized beds as is shown by figure 9. Even in a fluidized bed of 1.0 m dia. this characteristic non-uniformity is evident.

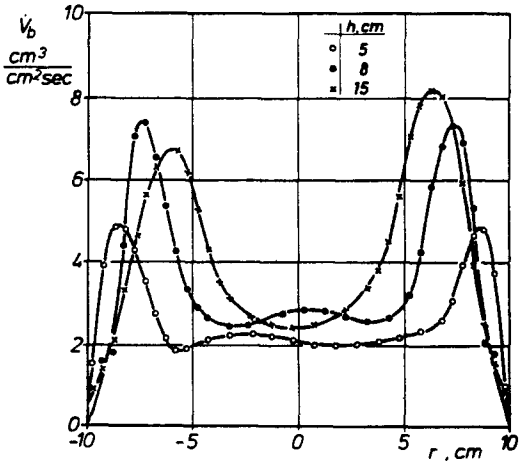

Figure 5. Variation of the local bubble gas flow with radial displacement of the probe from the vessel centre-line for different heights h above the distributor (0.20 m dia. sand fluidized bed, gas velocity 0.09 m/sec).

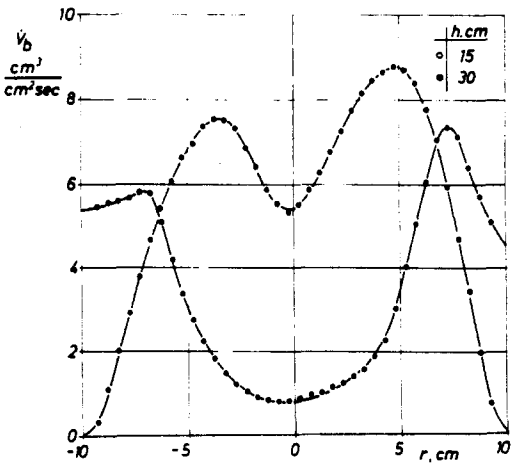

Figure 6. Variation of the local bubble gas flow with radial position of the probe for different heights h (glass spheres fluidized in the 0.20 m dia. bed, gas velocity 0.117 m/sec).

Summarizing, one may say that in all the fluidized bed systems investigated the bubble phase exhibited a characteristic flow profile possessing a zone of pronounced bubble development near the wall which moves to the centre of the vessel with height.

The non-uniformity of bubble development over the bed cross-section is so marked that its existence is detectable with comparatively inaccurate measuring techniques. For example, Park *et al.* (1969) detected a maximum in the bubble frequency near the distributor in a fluidized bed of 0.10 m dia. at value of r from between one-half and three-quarters of the bed radius. This maximum was found to move to the centre at larger heights. However, the dearth of accurate measuring techniques has prevented elucidation of the structure

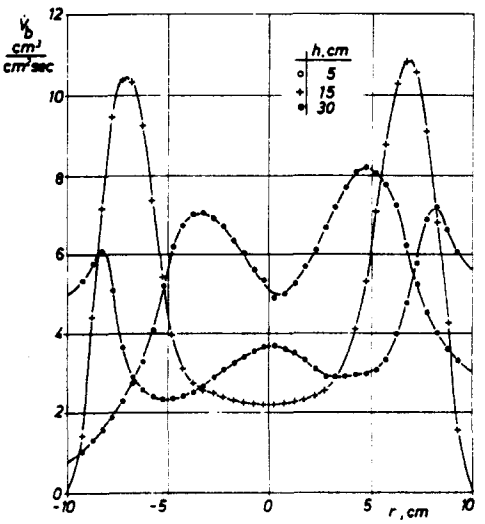

Figure 7. Variation of the local bubble gas flow with radial position of the probe for different heights h (copper powder fluidized in the 0.20 m dia. bed, gas velocity 0.084 m/sec).

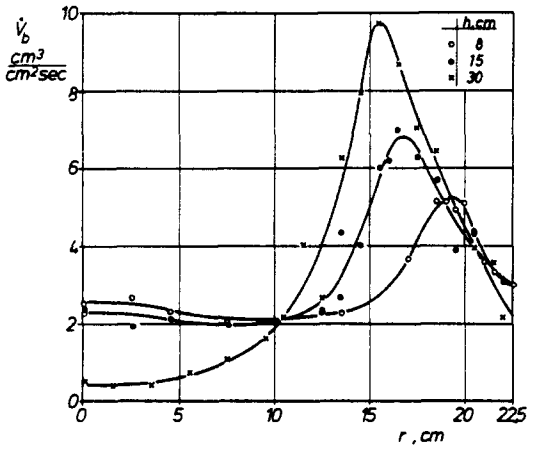

Figure 8. Variation of the local bubble gas flow with radial position of the probe for different heights h (0.45 m dia. sand fluidized bed, gas velocity 0.09 m/sec).

of the spatial flow profile of the bubble phase and has led to incorrect conclusions. For example Kunii, Yoshida & Hiraki (1967) deduced from measurements taken with a capacitive probe similar to that used by Morse & Ballou (1951), that bubbles rise uniformly over the cross-section at the distributor. They further concluded that bubbles rise uniformly distributed over the bed cross-section to a height approximately equal to the bed diameter. Only at greater heights do they rise at the bed centre-line due to coalescence. The data presented have shown that this description is incorrect.

Grace & Harrison (1968) on the basis of visual observations of a two-dimensional bed (0.457 m wide, 0.019 m thick) reached the conclusion that bubble development was uniform at the distributor. They therefore interpreted the observed non-uniformity of bubble development at greater heights by means of a coalescence model that used, as a starting point, a uniform distribution of bubbles at the distributor. According to this model the existence of the annular zone of increased bubble development was associated with a corresponding impoverishment of the fluidized bed regions near the wall.

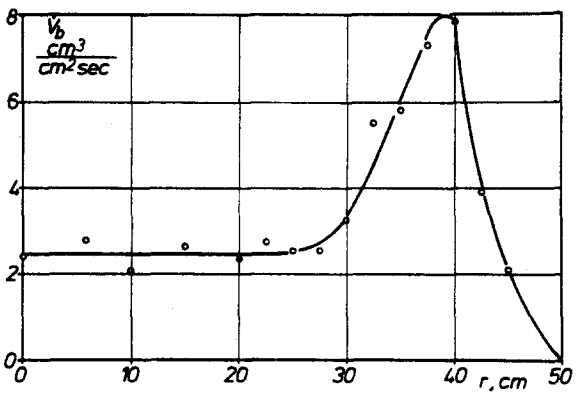

Figure 9. Variation of the local bubble gas flow with radial position of the probe in the 100 cm dia. sand fluidized bed (gas velocity 0.09 m/sec, probe located 0.30 m above the distributor).

If this model was correct, i.e. if the flow profile of the bubble phase did in fact start as uniform distribution, then the bubble gas flow averaged over a cross-section $\bar{\dot{V}}_b$ should exhibit approximately the same value as the local bubble gas flow $\dot{V}_b$ in the region of the bed not influenced by the proximity of the walls. Thus there should hold

$$\bar{\dot{V}}_b \cong \dot{V}_b|_{r=0}.$$

In fact it was found for example in a 0.20 m dia. bed of fluidized sand (figure 5) that at $h = 0.05$ m $\dot{V}_b|_{r=0} = 2\ \mathrm{cm^3/(cm^2/sec)}$, $\bar{\dot{V}}_b = 2.99\ \mathrm{cm^3/(cm^2/sec)}$, and in a bed of fluidized sand, with a diameter of 0.45 m (figure 8), at $h = 0.08$ m $\dot{V}_b|_{r=0} = 2.5\ \mathrm{cm^3/(cm^2/sec)}$, $\bar{\dot{V}}_b = 3.53\ \mathrm{cm^3/(cm^2/sec)}$.

From this it follows that no impoverishment of the regions near the wall was associated with the maximum in the flow profile and that bubble formation was favored near the walls.

There is unfortunately no satisfactory answer available why the zone near the wall should favor bubble formation. Possible influences that come to mind are the altered packing geometry of the particle layers near the wall which in packed beds (Calderbank & Pogorski 1957) and liquid fluidized beds (Allen & Smith 1971) lead to an increased flow through this region, as well as the different conditions of friction within the fluidized solids and between solids and wall which might favor bubble formation in immediate proximity to the wall.

Investigating three-dimensional processes by two-dimensional models, is problematic due to wall effects—particularly in the case of non-uniformity of bubble development across the bed diameter. Since bubbles at the point of their formation have diameter from 0.3 to 0.5 cm (Werther & Molerus 1971), it follows that a two-dimensional bed 1.9 cm thick has to be considered three-dimensional close to the distributor. Therefore, along the entire bed perimeter bubbles rise at the proximity of the wall so that from the wide side of the bed uniform bubble development is observed visually.

The number of bubbles generated at the narrow sides is relatively insignificant. Thus, in this case, a two-dimensional model does not describe a three-dimensional bed accurately. Hence it possesses an unrealistic initial condition for the investigation of the spatial distribution of bubbles. Comparison of the data of Grace & Harrison (1968) with the data presented here confirms this conclusion since the bubble frequency and distribution of bubble gas flow over the bed cross-section, as measured by Grace & Harrison, exhibit weak maxima near the wall in contrast to the very definite maxima found here in three-dimensional beds. These weaker maxima arise because of an apparently uniform initial distribution of bubbles across the bed cross-section.

In figure 10 spherical-cap bubbles are drawn at the position of maximum bubble gas flow for various heights above the distributor in a 0.20 m dia. bed. The diameters of the bubbles correspond to the 50 per cent and the 84 per cent values of the local cumulative number distribution of the bubble sizes. It follows from this representation that the displacement of the annular zone of pronounced bubble development results from the growth of the bubbles with increasing height—the larger the bubbles the further the annular zone is forced towards the vessel centre-line.

The scope of the present work only covers fluidized beds with porous plate distributors.

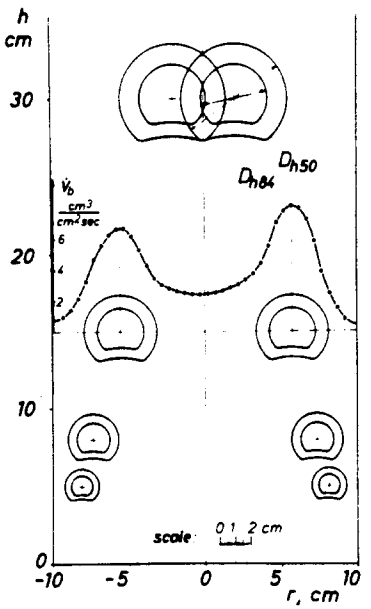

Figure 10. The relation between bubble coalescence and the variation of the bubble gas flow profile with height above the distributor. Bubble sizes corresponding to the 50 per cent and 84 per cent values of the local cumulative number distributions of bubble sizes are plotted at the position of maximum bubble gas flow in the corresponding bed cross-section (0.20 m dia. sand fluidized bed, gas velocity 0.09 m/sec).

Whitehead & Young (1967) reported investigations on a large scale fluidized bed of square cross-section of 1.20 × 1.20 m. Fluidizing air was fed via 16 nozzles while the solid (quartz sand. u_{mf} = 0.0245 m/sec) was fluidized at a velocity of 0.145 m/sec. The bubble eruption pattern at the bed surface was photographed for different bed depths. Figure 11 was derived from figures of the authors, where the positions of the eruption centres at the bed surface were plotted for various bed depths. As indicated by a comparison of figure 11 and figures 5–9 the characteristic flow profile is evident. Near the distributor at a height of 82.5 cm, a zone of pronounced bubble development is clearly distinguishable. This zone moves toward the centre with increasing height, and reaches the centre at a height of 2.03 m.

3.2. *The transition to the state of slugging*

The bubble development in a fluidized bed of quartz sand 0.10 m dia., is shown in figure 12. The annular zone of increased bubble development is clearly distinguishable for a height of 0.05 m above the distributor. This zone rapidly moves to the vessel centre. At a height of 15 cm it has almost reached the centre and at a height of 30 cm the characteristic flow pattern for narrow, high fluidized beds has developed, viz. the bubbles rise preferentially at the vessel centre. Figure 13 shows that the same flow pattern also arises with other solids.

The merging of the annular zone represents the start of the transition of the bed to the state of slugging. This is clear from an analysis of figures 14 and 15. In figure 14 the local

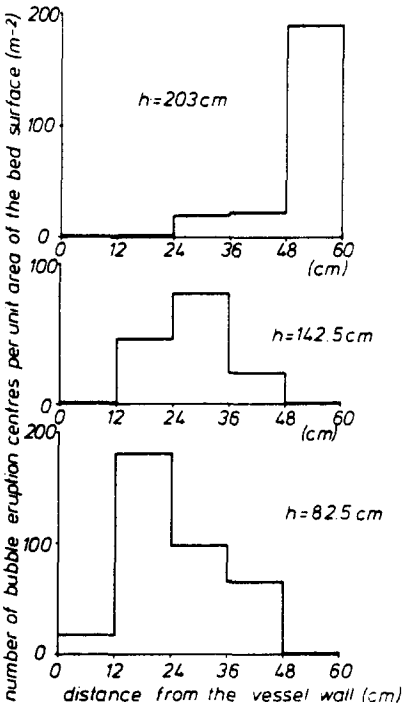

Figure 11. The bubble gas flow profile as deduced from measurements of Whitehead & Young (1967).

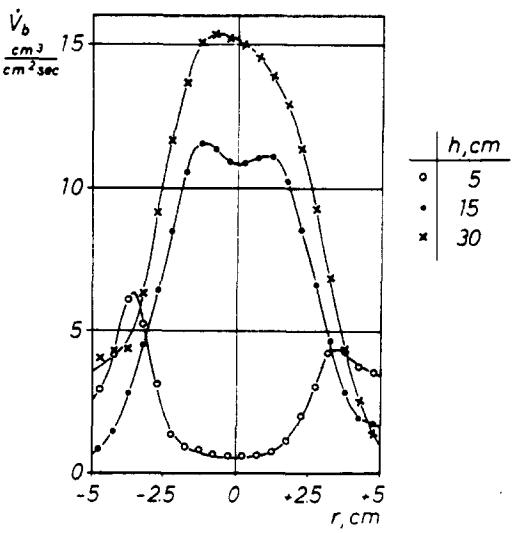

Figure 12. Variation of the local bubble gas flow with radial position of the probe (0.10 m dia. sand fluidized bed, gas velocity 0.09 m/sec).

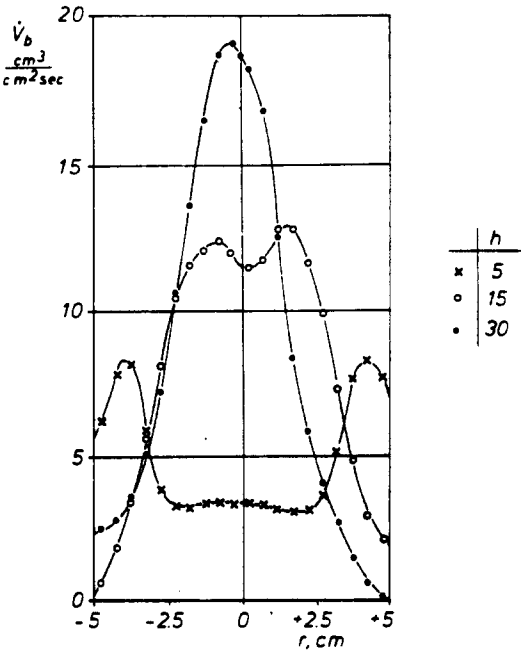

Figure 13. Variation of the local bubble gas flow with radial position of the probe (copper powder fluidized in the 0.10 m dia. bed, gas velocity 0.084 m/sec).

mean bubble rise velocity $\bar{v}_b$, the local mean pierced length $E[l]$ and the number k of bubbles striking the probe per unit time are plotted versus r, the distance from the vessel centre, for heights of 0.225, 0.30 and 0.80 m above the distributor. In figure 15 the variation with height of the local magnitudes of $\bar{v}_b$ and $E[l]$ at the vessel centre-line are shown.

It is evident that at a height of 0.225 m above the distributor the bubbles are still relatively small, that they rise preferentially at the centre and that in the bubble track thus formed at the centre-line the bubbles achieve very high rise velocities.

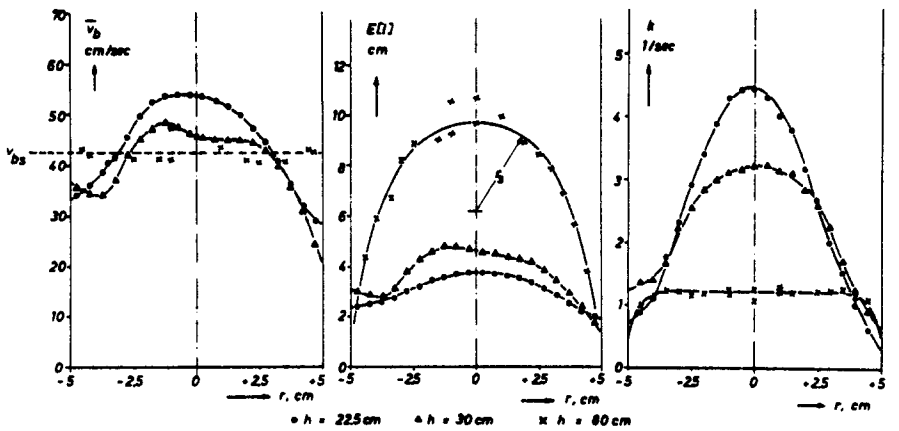

Figure 14. The transition into the slugging state (0.10 m dia. sand fluidized bed, gas velocity 0.09 m/sec).

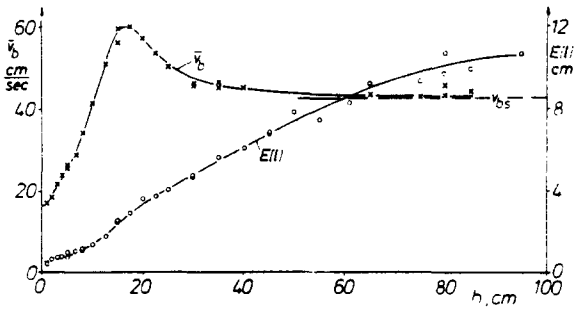

Figure 15. Variation of local mean bubble rise velocity and local mean bubble pierced length with height above the distributor (0.10 m dia. sand fluidized bed, gas velocity 0.09 m/sec, probe located in the column axis).

Due to the high bubble concentration at the centre-line the bubbles coalesced very rapidly so that at a height of 30 cm a changed flow pattern is recognizable. In particular, the number of bubbles striking the probe per unit time k declined. The bubbles are larger but the local mean bubble rise velocities have decreased due to increasing wall effects. With increasing height above the distributor the characteristic profile for slugging fluidized beds becomes more clearly apparent. At a height of 80 cm the local rise velocity is close to uniform over the bed cross-section and agrees quite well with the predicted value for slugging fluidized beds (Hovmand & Davidson, 1971), according to

$$v_{bs} = u_o - u_{mf} + 0.35\sqrt{gD_B} \qquad [5]$$

where u_o is the superficial gas velocity, D_B is the bed diameter and v_{bs} is the absolute rise velocity of a slug. For the present example this value is $v_{bs} = 0.423$ m/sec. The magnitude k also possesses an almost constant value across the bed diameter as would be expected in this case, since the maximum horizontal diameter of the rising bubbles is only a little less than the vessel diameter.

For a fully developed slugging fluidized bed where all slugs possess the same shape and rise centred on the vessel axis, the measurements of the local mean pierced lengths plotted versus r, the distance from the centre-line give an insight into the shape of the slugs. Since it is known from the X-ray photographs of Ormiston, Mitchell & Davidson (1965), that the trailing surface of slugs is flat at least near the centre-line, the plot of $E[l]$ as a function of r is, at least in that region, identical to a vertical section through a slug of average size. The radius of curvature r_s of the slug, at the stagnation point was measured by Ormiston, Mitchell & Davidson (1965):

$$r_s = 0.35\, D_B. \qquad [6]$$

Using $D_B = 0.10$ m the computed radius of curvature r_s approximates the measured values of $E[l]$ quite well near the vessel centre-line for a height of 80 cm. In summary, the data represented in figures 14 and 15 prove that the merging of the annular zone signifies the start of the transition of the fluidized bed to the state of slugging.

It is significant however, that even a slugging fluidized bed which is characterized by bubbles rising at the vessel centre-line, possesses a region near the distributor where the

bubbles rise preferentially at the wall. It was evident that this region in which the bubbles are small compared to the vessel diameter, and where therefore quite different exchange behavior exists compared to the slugging region, had an accurately definable, non-negligible size. The existence of this region of intense contact should be allowed for in the design of slug-flow reactors.

3.3. *The influence of the flow profile of the bubble phase on solids circulation and gas mixing*

The fundamental investigations of Rowe and co-workers (1962, 1965, 1971) have shown that the bubbles rising in a fluidized bed cause not only an upwards drift of surrounding solid particles but also carry up solids in their wakes. From this it follows directly that a non-uniformity of bubble development over the bed cross-section must necessarily be the cause of a macroscopic solids circulation. In regions of more intense bubble development, solids are carried up and therefore because of continuity, must move downwards in regions of lesser bubble activity. If the down flow of solids is sufficiently intense, the particles descend at a velocity greater than the interstitial velocity of fluidizing gas. The resulting backmixing of the gas phase is significant in the operation of a catalytic fluidized bed reactor and has been accounted for by the countercurrent backmixing model suggested by several authors (Stephens, Sinclair & Potter 1967; Van Deemter 1967; Latham, Hamilton & Potter 1968; Kunii & Levenspiel 1969).

It is possible to predict the solids circulation. Since the solids carried by the bubbles in their wakes are deposited at the bed surface, the eruption pattern at this surface or the flow profile of the bubble phase close to the surface is decisive in determining the large scale solids circulation.

The annular zone of pronounced bubble development merges approximately at a height of two bed diameters above the distributor at the vessel centre-line. In fluidized beds deeper than two bed diameters, the bubbles break the surface preferentially at the centre. The solids carried up by the bubbles descend mainly near the wall. The solids circulation is such that the solids rise first in the annular zone of increased bubble development, then in the centre and subsequently descend near the wall. Such a circulation pattern—rising in the centre, descending at the wall—which has already been observed repeatedly in laboratory fluidized beds (Leva 1962; Potter 1971; Schügerl 1967), is schematically shown in figure 16a.

On the other hand, a fluidized bed shallower than about two bed diameters exhibited a completely different solids circulation pattern (figure 16b). In that case the eruption pattern is determined by the annular zone of increased bubble development. The solids falling on the bed surface may either descend at the bed centre or at the wall, i.e. two downflows of solids are set up. Such a circulation pattern predicted merely from a knowledge of the spatial bubble flow profile has been experimentally observed by Whitehead, Gartside & Dent (1970) in a large-scale bed of square cross-section with an edge length of 1.20 m. The existence of a downflow of solids at the vessel centre-line has been deduced by Calderbank, Toor & Lancaster (1967) from experiments on a catalytic fluidized bed reactor with a diameter of 0.45 m. The quantitative distribution of the solids between the two downflows should be dependent on the distance of the annular zone from the vessel centre-line and

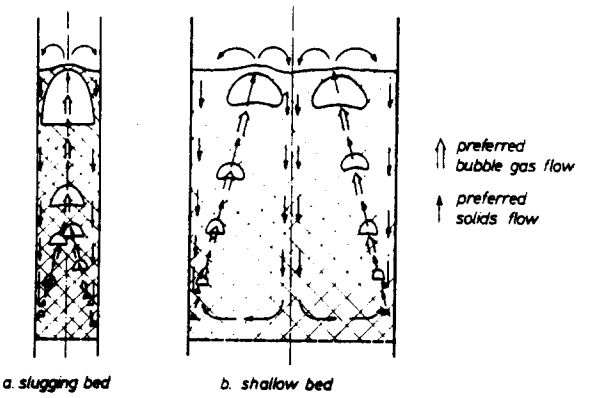

Figure 16. The development of different solids circulation patterns in beds of different height-to-diameter ratios.

consequently on the ratio of bed height to diameter. The limiting case then results when the annular zone has reached the centre, i.e. the pattern is achieved where solids are rising at the centre and descending at the wall, as shown in figure 16a.

4. SUMMARY AND CONCLUSIONS

The newly developed measuring techniques were used for investigating the spatial distribution of bubbles in cylindrical fluidized beds with diameters of 0.10 to 1.0 m. The results indicate that in gas/solid fluidized beds, close to the distributor a zone of increased bubble development exists in an annulus near the wall. This zone of higher bubble activity moves towards the vessel centre-line with increasing height above the distributor. Contrary to the qualitative observations available to date that initially the distribution of bubbles over the bed cross-section is uniform, it was found that the annular zone of higher bubble activity results from the fact that bubbles are formed preferentially in proximity to the walls.

The merging of the annular zone in the vessel centre-line marks the beginning of the transition of the fluidized bed to the state of slugging. Hydrodynamically, three different regions should be distinguished in a slugging fluidized bed:

(i) a region near the distributor characterized by the existence of an annular zone of increased bubble development;
(ii) a transition region starting at the point at which the annular zone coalesces on the bed centre-line; and
(iii) the region of fully developed slugging.

As is shown by a comparison with the data of Whitehead and co-workers, the same flow profile of the bubble phase also exists in industrial-scale fluidized beds, i.e. the flow patterns determined here are of general nature.

It is shown that a knowledge of the spatial flow profile of the bubble phase is the key to an understanding of the solids circulation within the fluidized bed. The flow profile of the bubble phase induces the large scale solids circulation in the bed in a manner dependent on the ratio of bed depth to diameter, i.e. on the extent to which the development of the

flow profile has advanced at the bed surface. The solids circulation then in turn, influences solids and gas mixing within the fluidized bed.

Acknowledgement—The authors thank the Deutsche Forschungsgemeinschaft (DFG) for financial support of this work.

REFERENCES

ALLEN, B. G. & SMITH, J. W. 1971 Fluid velocity profiles near the wall of liquid-fluidized beds. *Can. J. Chem. Engng* **49**, 430–438.

BAUMGARTEN, P. K. & PIGFORD, R. L. 1960 Density fluctuations in fluidized beds. *A.I.Ch.E.J.* **6**, 115–126.

CALDERBANK, P. H. & POGORSKI, L. A. 1957 Heat transfer in packed beds. *Trans. Inst. Chem. Engrs* **35**, 195–207.

CALDERBANK, P. H., TOOR, F. D. & LANCASTER, F. H. 1967 Reaction kinetics in gas-fluidized catalyst beds—experimental. *Proceedings of the International Symposium on Fluidization*, p. 652. Eindhoven.

GRACE, J. R. & HARRISON, D. 1968 The distribution of bubbles within a gas-fluidized bed. *Inst. Chem. Engrs Symp. Ser.* **30**, 105–125.

HOVMAND, S. & DAVIDSON, J. F. 1971 Slug flow reactors. In: *Fluidization*, p. 193. (Eds J. F. Davidson & D. Harrison). Academic Press.

KUNII, D., YOSHIDA, K. & HIRAKI, I. 1967 The behaviour of freely bubbling fluidized beds. *Proceedings of the International Symposium on Fluidization*, p. 243. Eindhoven.

KUNII, D. & LEVENSPIEL, O. 1969 *Fluidization Engineering*. Wiley.

LATHAM, R., HAMILTON, C. & POTTER, O. E. 1968 Back-mixing and chemical reaction in fluidized beds. *Br. Chem. Engng* **13**, 666–681.

LEVA, M. 1962 The use of gas-fluidized systems for blending particulate solids, *Symp. Interaction between fluids and particles*, p. 143. Inst. Chem. Engrs.

MORSE, R. D. & BALLOU, C. O. 1951 The uniformity of fluidization, its measurement and use. *Chem. Engng Progr.* **47**, 199–219.

ORMISTON, R. M., MITCHELL, F. R. G. & DAVIDSON, J. F. 1965 The velocities of slugs in fluidized beds. *Trans. Inst. Chem. Engrs* **43**, 209–230.

PARK, W. H., KANG, W. K., CAPES, C. E. & OSBERG, G. L. 1969 The properties of bubbles in fluidized beds of conducting particles as measured by an electroresistivity probe. *Chem. Engng Sci.* **24**, 851–869.

POTTER, O. E. 1971 Mixing. In: *Fluidization*, p. 293. (Eds J. F. Davidson & D. Harrison). Academic Press.

ROWE, P. N. & PARTRIDGE, B. A. 1962 Particle movement caused by bubbles in a fluidized bed. *Symp. Interaction between Fluids and Particles*, p. 135. Inst. Chem. Engrs.

ROWE, P. N., PARTRIDGE, B. A., CHENEY, A. G., HENWOOD, G. A. & LYALL, E. 1965 The mechanisms of solids mixing in fluidized beds. *Trans. Inst. Chem. Engrs* **43**, 271.

ROWE, P. N. 1971 Experimental properties of bubbles. In: *Fluidization*, p. 121. (Eds J. F. Davidson & D. Harrison). Academic Press.

SCHÜGERL, K. 1967 Comment, *Proceedings of the International Symposium on Fluidization*, p. 662. Eindhoven.

STEPHENS, G. K., SINCLAIR, R. J. & POTTER, O. E. 1967 Gas exchange between bubbles and dense phase in a fluidized bed. *Powder Tech.* **1**, 157–178.

VAN DEEMTER, J. J. 1967 The counter-current flow model of a gas–solids fluidized bed. *Proceedings of the International Symposium on Fluidization*, p. 334, Eindhoven.

WERTHER, J. & MOLERUS, O. 1971 Autokorrelation und Kreuzkorrelation zur Messung lokaler Blasengrößen und -aufstiegsgeschwindigkeiten in realen Gas/Feststoff-Fließbetten. *Chemie-Ing.-Techn* **43**, 271–288.

WERTHER, J. 1973 Bubbles in gas fluidized beds, to be published.

WHITEHEAD, A. B. & YOUNG, A. D. 1967 Fluidization performance in large scale equipment: Part I. *Proceedings of the International Symposium on Fluidization*, p. 284. Eindhoven.

WHITEHEAD, A. B., GARTSIDE, G. & DENT, D. G. 1970 Flow and pressure maldistribution at the distributor level of a gas solid fluidized bed. *Chem. Engng J.* **1**, 175–190.

Sommaire—La répartition spatiale de bulles dans des bains fluides au gaz e été étudiée avec le système de mesure décrit dans la première partie de cet ouvrage dans des bains de 0,10, 0,20, 0,45 et 1,0 m de diamètre. Les résultats indiquent que dans des bains fluides au gaz un profil d'écoulement caractéristique de la phase en bulle existe de sorte que près du distributeur une zone de développement croissant de bulles existe dans un anneau près de la paroi. Cette zone se déplace vers l'axe du vaisseau à mesure que la hauteur au-dessus du distributeur augmente. Le fusionnement de la zone annulaire dans l'axe du vaisseau marque le début de la transition du bain fluide à l'état inerte. Le profil d'écoulement spatial de la phase en bulle est motré être responsable pour l'existence de modes de circulation de solides caractéristiques dans les bains fluides au gaz.

Zusammenfassung—Mit Hilfe des in Teil I dieser Veröffentlichung beschriebenen Meßsystems ist die räumliche Verteilung der Blasen in Fließbetten von 0,10, 0,20, 0,45 und 1,0 m Durchmesser untersucht worden. Die Messungen zeigen, daß in Gas/Feststoff-Fließbetten ein charakteristisches Strömungsprofil der Blasenphase existiert derart, daß in der Nähe des Aufgabebodens eine ringförmige, wandnahe Zone verstärkter Blasenentwicklung festgestellt wird. Diese Zone verschiebt sich mit zunehmender Höhe über dem Aufgabeboden zur Rohrmitte hin. Das Zusammenwachsen der Ringzone in der Rohrmitte markiert den Beginn des Überganges des Fließbettes in den Zustand des Stoßens. Es wird gezeigt, daß dies räumliche Strömungsprofil der Blasenphase die Ursache für die Existenz charakteristischer Feststoffzirkulationsströmungen in Gas/Feststoff-Fließbetten ist.

Резюме—Системой измерения, описанной в первой части этой работы, исследовалось пространственное распределение пузырьков в флюидизированных слоях газа диаметрами 0,10; 0,20; 0,45 и 1,0 м. По результатам видно, что в слоях флюидизированного газа характерный профиль течения пузырьков фазы таковой, что вблизи распределительного устройства в кольцеобразном слое около стены существует зона повышенного развития пузырьков. Эта зона передвигается к оси сосуда наверх от распределительного устройства. Слитие кольцеобразного слоя с осью сосуда отмечает начало перехода флюидизированного слоя в состояние инертности. Нашли, что пространственный профиль течения фазы пузырьков является причиной существования характерной циркуляции твердых частиц в слоях флюидизированного газа.